Analyst

PAPER

View Article Online
View Journal



Cite this: DOI: 10.1039/c5an00107b

# Aptamer-based colorimetric biosensing of abrin using catalytic gold nanoparticles†

Jingting Hu,[a,b] Pengjuan Ni,[a,b] Haichao Dai,[a,b] Yujing Sun,[a] Yilin Wang,[a,b] Shu Jiang[a,b] and Zhuang Li*[a]

Received 18th January 2015,
Accepted 19th March 2015

DOI: 10.1039/c5an00107b

www.rsc.org/analyst

In this study we propose a simple and sensitive colorimetric aptasensor for the quantitative analysis of abrin by using catalytic AuNPs for the first time. AuNPs possess the peroxidase-like activity that can catalyse 3,3,5,5-tetramethylbenzidine (TMB) in the presence of $H_2O_2$, leading to color change of the solution. It is interesting to find that the peroxidase-like activity of AuNPs can be improved by surface activation with a target-specific aptamer. However, with a target molecule, the aptamer is desorbed from the AuNPs surface, resulting in a decrease of the catalytic abilities of AuNPs. The color change of the solution is relevant to the target concentration, and this can be judged by the naked eye and monitored by using a UV-vis spectrometer. The linear range for the current analytical system was from 0.2 nM to 17.5 nM. The corresponding limit of detection (LOD) was 0.05 nM. Some other proteins such as thrombin (Th), glucose oxidase (GOx), and bovine serum albumin (BSA) all had a negligible effect on the determination of abrin. Furthermore, several practical samples spiked with abrin were analyzed using the proposed method with excellent recoveries. This aptamer-based colorimetric biosensor is superior to other conventional methods owing to its simplicity, low cost, and high sensitivity.

## 1. Introduction

Abrin is a highly toxic protein which is found in the beans of *Abrus precatorius*. Along with ricin, it belongs to the type II ribosome inactivating protein family.[1] Abrin has been found to be more toxic than its counterpart ricin, with a human lethal dose of 0.1–1 μg $kg^{-1}$ [2] as compared to 5–10 μg $kg^{-1}$ for ricin inhalation.[3] The abrin toxin consists of two non-identical polypeptide chains (A and B) cross linked by a single disulfide bond. The A-chain is an efficient *N*-glycosidase and is transported across the plasma membrane by the B-chain *via* endocytosis into the cytoplasm of cells. Once internalized, the A-chain removes an adenine from an exposed loop of 28S ribosomal RNA, thus inhibiting protein synthesis and resulting in eventual cell death.[4–7] Abrin should be closely monitored as a threatening biological agent due to its easy cultivation and cheap preparation, and it is included in the Biological and Toxin Weapons Convention (BTWC) Procedural Report (2001).[8] Hence, the research studies focused on rapid detection and specific recognition of the abrin toxin should be paid more attention.

Several technologies have been developed for abrin detection, including surface-enhanced Raman spectroscopy,[9] electrochemiluminescence assays,[10] liquid chromatography tandem mass spectrometry (LC/MS),[11] and antibody-based immunoassays.[12,13] Although, these assays are effective for abrin detection, most of these analytical methods rely on sophisticated instruments and skilled manpower, making such approaches impractical for on-site detection.

Of the alternatives to antibody-based sensing assays, aptamer-based methods have become popular over the past few decades due to their inherent selectivity, affinity, and multifarious advantages over the traditional recognition elements. As a new class of single-stranded DNA/RNA molecules, aptamers are selected *in vitro* by the systematic evolution of the ligand by the exponential enrichment (SELEX) process from random-sequence nucleic acid libraries. These molecular ligands have the ability to recognize their cognate targets with high affinity and specificity. This property makes aptamers an ideal tool to detect a variety of target molecules including proteins, drugs, small molecules, inorganic ions and even cells.[14–19]

Nowadays, increasing attention has been paid to the nanoscaled peroxidase mimetics and their potential applications in bioanalysis[20–26] since the first $Fe_3O_4$ magnetic nanoparticle-based peroxidase was reported.[27] A variety of nanomaterials

[a]State Key Laboratory of Electroanalytical Chemistry, Changchun Institute of Applied Chemistry, Chinese Academy of Sciences, Changchun, Jilin 130022, PR China
[b]University of Chinese Academy of Sciences, Beijing, 100039, PR China.
E-mail: zli@ciac.jl.cn; Fax: +86 431 85262057; Tel: +86 431 85262057

†Electronic supplementary information (ESI) available. See DOI: 10.1039/c5an00107b

have also been demonstrated to possess intrinsic peroxidase-like activity. Although gold is usually viewed as an inert metal, surprisingly it has been found that AuNPs possess intrinsic peroxidase-like activity.[28,29] The findings show that a catalytic AuNP-based strategy has enormous potential in detection and can be exploited to develop biosensors for a wide variety of target analytes.

Enlightened by the above facts, we propose an aptamer-based colorimetric biosensor of abrin based on the peroxidase-like activity of gold nanoparticles. An abrin binding aptamer (ABA) can be absorbed onto the surface of AuNPs and improve the ability of AuNPs to catalyze 3,3,5,5-tetramethylbenzidine (TMB) in the presence of $H_2O_2$ and lead to significant enhancement of the absorbance. However, in the presence of abrin, the ABA undergoes target-responsive structural changes followed by desorption from the AuNPs surface to allow an aptamer-target binding event, resulting in a decrease in the catalytic abilities of AuNPs. The highly selective and sensitive detection of abrin is possible using the naked eye or monitored by using an UV-vis spectrometer. Furthermore, the proposed method does not require any modification of the aptamer, making it time-saving and cost-effective.

## 2. Experimental

### 2.1. Reagent and chemicals

Abrin was purchased from Beijing Hapten and Protein Biomedical Institute (Beijing, China). The sequence of the abrin binding aptamer (ABA) was 5′-ATCCTGTGAGGAATGCTCATGCATAGCAAGGGCT-3′.[30] The ssDNA oligonucleotides were synthesized by Shanghai Sangon Biotechnology Co. Ltd (Shanghai, China) and the lyophilized powder was dissolved in distilled water and before use it was stored at 4 °C. The concentration of the oligonucleotide was determined by measuring the UV absorbance at 260 nm. Chloroauric acid ($HAuCl_4{\cdot}4H_2O$) was obtained from Shanghai Chemical Reagent Company (Shanghai, China). 3,3,5,5-Tetramethylbenzidine (TMB) and hexadecyltrimethylammonium bromide (CTAB) were purchased from Aladdin Reagent Company (Shanghai, China). Thrombin (Th), glucose oxidase (GOx), and bovine serum albumin (BSA) were purchased from Sigma-Aldrich Chemical Co. (Milwaukee, WI, USA). $C_6H_5Na_3O_7$, $H_2O_2$, $Na_2HPO_4{\cdot}12H_2O$ and $NaH_2PO_4{\cdot}2H_2O$ were obtained from Beijing Chemical Reagent Company. All of the reagents were of analytical grade and used as received. Ultrapure water obtained from a Millipore water purification system (≥18 MΩ, Milli-Q, Millipore) was used in all runs.

### 2.2. Instrumentation

The ultraviolet-visible (UV-vis) absorption spectra were recorded on a Cary 50 Scan UV-vis spectrophotometer (Varian, USA) at 25 °C. The zeta potentials were measured on Malvern Zetasizer Nanoseries at 25 °C. Transmission electron microscopy (TEM) measurements were made on a Hitachi H-8100 transmission electron microscope operated at an accelerating voltage of 100 kV.

### 2.3. Synthesis of the citrate-protected AuNPs

AuNPs were synthesized using the classical citrate reduction method.[31] Briefly, colloidal AuNPs with an average diameter of 13 nm were prepared by rapidly injecting a sodium citrate solution (10 mL, 38.8 mM) into a boiling aqueous solution of $HAuCl_4{\cdot}4H_2O$ (100 mL, 1 mM) with vigorous stirring. After boiling for 30 min, the reaction flask was removed from the heat to allow the reaction solution to cool at room temperature. The concentration of the AuNPs was about 10 nM, which was determined according to Beer's law by using the extinction coefficient of $2.78 \times 10^8$ $M^{-1}$ $cm^{-1}$ for 13 nm AuNPs in diameter at 520 nm.[32]

### 2.4. Detection of abrin using the colorimetric biosensing method

A typical colorimetric analysis was realized by the following procedure: first, 100 μL of 2.5 nM 13 nm AuNPs was mixed with 20 μL of 5 μM ABA. Second, 50 μL abrin with an appropriate concentration in PB (pH 7.4) was added to the AuNPs/ABA solution. The solutions were allowed to react for 5 min and then 15 μL of 10 mM TMB and 15 μL of 10 M $H_2O_2$ were added to produce the color change. The solution was equilibrated for 10 min at 25 °C, and then was transferred to a quartz cuvette. The UV–vis absorption spectra were recorded over wavelengths ranging from 550 nm to 750 nm.

### 2.5. Treatment of raw milk

Milk samples were prepared by following the previous method with a minor modification.[33] Briefly, 5.0 mL of raw milk was placed in a 7 mL centrifuge tube, and 1.5 mL of 2 M trichloroacetic acid was added. After ultrasonication for 10 min, the mixture was centrifuged at 10 000 rpm for 10 min.

## 3. Results and discussion

### 3.1. The mechanism of the sensing system

Recently, it has been demonstrated that the peroxidase-like activity of nanoparticles varied with respect to electrostatic affinity between nanoparticles and substrates. Two substrates would be helpful to evaluate this point of view.[34,35] ABTS (negatively charged) possesses two sulfonic acid groups, exhibiting higher affinity toward a positively charged nanoparticle surface. With ABTS as the substrate, cationic nanoparticles displayed a high affinity and subsequently a high peroxidase activity. Conversely, TMB (positively charged) carries two amine groups, exhibiting stronger affinity toward a negatively charged nanoparticle surface. With TMB as a substrate, anionic nanoparticles had a high affinity and exhibited a high catalytic activity.

As mentioned above, Fig. 1 outlines the concept of the catalysis-based colorimetric assay. According to previous reports,[36,37] a random coil ssDNA (ABA herein) could uncoil sufficiently to expose its bases, which could be easily adsorbed onto the surface of AuNPs. Thus, the DNA phosphate backbone with a large number of negative charges existed on the

 

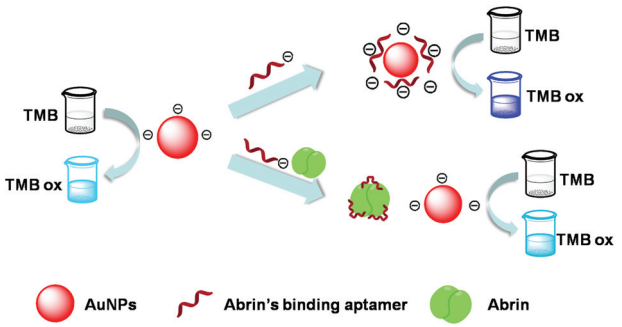


Fig. 1 The mechanism of the aptamer-based colorimetric biosensor for abrin.

surface of AuNPs. Therefore, with positively charged TMB as a substrate, the ABA–AuNP complex had a high affinity and exhibited a significant enhancement of catalytic activity. However, upon the addition of abrin, ABA bound to abrin followed by desorption from the AuNPs surface and the conformation of ABA was changed from the random coil structure to a G-quadruplex structure (rigid structure). The rigid structure prevented the exposure of the ABA bases to AuNPs and the negative charges existing on the surface of AuNPs were less, resulting in a decrease of the catalytic abilities of AuNPs.

### 3.2. Spectral characteristics

To confirm the feasibility of our concept, the spectral responses of the aptamer-based colorimetric biosensor were observed under different conditions (Fig. 2A). The spectral value of AuNPs alone in solution at 650 nm was 0.8 absorbance units (a.u.) (1, Fig. 2A), which can be explained by the oxidation of colorless TMB to blue TMB ox by catalysis. In the presence of ABA, this value (2, Fig. 2A) increased to 1.25 a.u., indicating the enhancement of catalysis of AuNPs. When abrin molecules were present in the solution (3, Fig. 2A), ABA bound to abrin followed by desorption from the AuNPs, resulting in a decrease of the catalytic abilities of AuNPs. As expected, the addition of abrin alone did not cause the color change of the solution (4, Fig. 2A) compared with AuNPs alone (1, Fig. 2A). Furthermore, the spectral value of AuNPs in the presence of CTAB (a kind of cationic surfactant) at 650 nm was 0.3 (5, Fig. 2A). These results confirm that the negatively charged aptamer is the main cause of the enhancement of AuNP-dependent catalysis. Table 1 shows the zeta potential of AuNPs under different conditions and the results are in agreement with our mechanism.

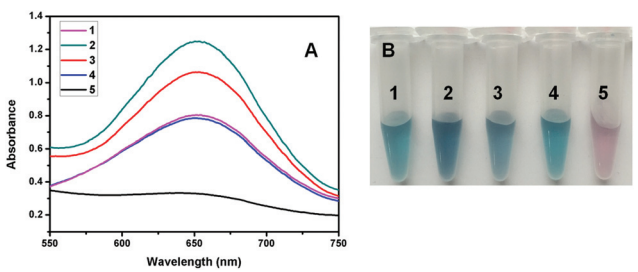


Fig. 2 (A) UV-vis spectra in the presence of TMB and $H_2O_2$ under different conditions of (1) 1.3 nM AuNPs, (2) 1.3 nM AuNPs + 0.5 μM ABA, (3) 1.3 nM AuNPs + 0.5 μM ABA + 1 nM abrin, (4) 1.3 nM AuNPs + 1 nM abrin, (5) 1.3 nM AuNPs + 0.3 g $L^{-1}$ CTAB. (B) The corresponding digital images.

Table 1 Zeta potential of AuNPs under different conditions

| Sample | Zeta potential (mV) |
|---|---|
| AuNPs[a] | −8.58 |
| AuNPs[a] + ABA[b] | −16.00 |
| AuNPs[a] + ABA[b] + abrin[c] | −11.10 |
| AuNPs[a] + CTAB[d] | 1.03 |

[a] $C_{AuNPs}$ = 1.3 nM. [b] $C_{ABA}$ = 0.5 μM. [c] $C_{Abrin}$ = 1 nM. [d] $C_{CTAB}$ = 0.3 g $L^{-1}$.

In order to get rid of the possible impact of oxidation of TMB caused by ABA, abrin, and the abrin–ABA complex, these three molecules were also employed in the oxidation of TMB (Fig. S1†). The results indicate that ABA, abrin, and the abrin–ABA complex do not possess the peroxidase-like activity. Fig. S2† shows the morphological characteristics of AuNPs under different conditions. The AuNPs are monodisperse and spherical with an average size of 13 nm (Fig. S2†). The UV-visible spectra of AuNPs, AuNP–ABA, AuNP–abrin and AuNP–ABA–abrin complex show typical Au NP SPR peaks with maxima at 520 nm, confirming the stability of AuNPs under different conditions (Fig. S3†). The observation showed that there was no aggregation of AuNPs caused by ABA, abrin and the ABA–abrin complex.

### 3.3. Optimization of the key parameters

The peroxidase-like activity of AuNPs depends on some key parameters, such as the concentration of ABA, TMB and $H_2O_2$, reaction time, temperature, pH value and the size of AuNPs. Therefore, these key parameters were optimized prior to the application of our proposed method. We used the reduction of absorbance, that is, $A_0 - A$ ($\Delta A$) as a criterion to optimize the detection conditions. $A_0$ presents the absorbance at 650 nm in the absence of abrin. $A$ presents the absorbance at 650 nm in the presence of 5 nM abrin.

**3.3.1. Effect of reaction time.** Fig. S4† shows the effect of reaction time on the peroxidase-like activity of the sensing system. It is shown that $\Delta A$ reaches a plateau from 10 to 20 min. Accordingly, 10 min was chosen as the reaction time (ESI, Fig. S4†).

**3.3.2. Effect of reaction temperature.** Temperature is another crucial factor for most enzyme-based systems. Fig. S5† shows that $\Delta A$ increases with increasing temperature in the range from 15 °C to 25 °C. Further increase in temperature results in the decrease of $\Delta A$. Therefore, 25 °C was chosen as the reaction temperature (ESI, Fig. S5†).

**3.3.3. Effect of ABA concentration.** Fig. S6† displays the effect of ABA concentration on the sensing system. It is clearly seen from Fig. S6† that the concentration of ABA being too high or too low is not suitable for improving the sensitivity. $\Delta A$ is reduced with increasing ABA concentration in the range from 0.5 μM to 0.7 μM and this fits the theory that abrin competes with AuNPs for binding to ABA and the least surface activated AuNP amount of ABA means the most sensitivity. However, 0.2, 0.3, and 0.4 μM ABA are too small to improve the peroxidase-like activity of AuNPs. Hence, the concentration of ABA was selected to be 0.5 μM for this experiment (ESI, Fig. S6†).

**3.3.4. Effect of $H_2O_2$ and TMB concentration.** The impact of TMB and $H_2O_2$ concentration on the sensitivity of the sensing system was examined. Fig. S7† shows that $\Delta A$ increased with increasing $H_2O_2$ concentration from 0.3 M to 0.75 M and then it reduces with increasing $H_2O_2$ concentration in the range from 0.75 M to 1 M. Fig. S8† shows that $\Delta A$ increased with increasing TMB concentration from 0.3 mM to 0.75 mM and then it reduces with increasing TMB concentration in the range from 0.75 mM to 1 mM. These results suggest that the reaction of $H_2O_2$ with TMB catalyzed by AuNPs reached equilibrium when the concentrations of $H_2O_2$ and TMB were 0.75 M and 0.75 mM. Therefore, 0.75 M of $H_2O_2$ and 0.75 mM of TMB were chosen for the next experiments (ESI, Fig. S7 and S8†).

**3.3.5. Effect of pH value.** pH is a crucial factor for almost every sensing system. Fig. S9† displays the effect of pH value on the sensing system. It is shown that $\Delta A$ increases with increasing pH value in the range from 6.2 to 7.4. Further increase of pH value results in the decrease of $\Delta A$. Therefore, pH 7.4 was adopted in the following experiments (ESI, Fig. S9†).

**3.3.6. Effect of the size of AuNPs.** Fig. S10† shows the morphological characteristics of AuNPs with different sizes (13 nm, 25 nm and 40 nm) and Fig. S11† shows the effect of AuNP size on the sensing system. The results show that $\Delta A$ for 13 nm, 25 nm and 40 nm AuNP solution is 0.292, 0.212, 0.182, respectively, under similar experimental conditions. Thus, we used 13 nm AuNPs as the following experimental conditions on the basis of higher sensitivity (ESI, Fig. S10 and S11†).

### 3.4. Colorimetric biosensing of abrin

Under the optimal detection conditions, the peroxidase-like activities of the AuNPs on TMB oxidation in the presence of various concentrations of abrin were investigated. The $\Delta A$ at 650 nm in the presence of different amounts of abrin is shown in Fig. 3A. The digital images show that with increasing abrin concentration, the color of the solution changed from dark blue to light blue, suggestive of the abrin concentration-dependent TMB catalysis. It can be evidently observed that the $\Delta A$ at 650 nm increases gradually with increasing concentration of abrin. In other words, with increasing concentration of abrin, the peroxidase-like activities of AuNPs decreased. This observation is in accord with our hypothesis. As shown in Fig. 3B, $\Delta A$ exhibits a good linear relationship with $\log C$ (abrin, nM)

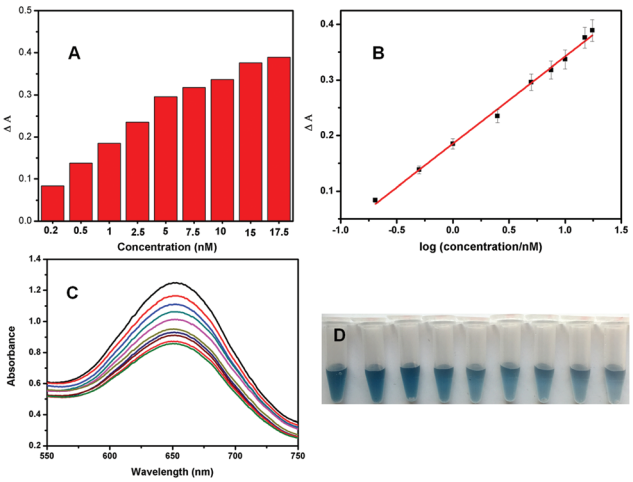


**Fig. 3** (A) $\Delta A$ at 650 nm in the presence of various concentrations of abrin. (B) Typical calibration curve for abrin obtained using the aptamer-based colorimetric biosensor. (C) UV-vis spectra in the presence of various concentrations of abrin (0 nM, 0.2 nM, 0.5 nM, 1 nM, 2.5 nM, 5 nM, 7.5 nM, 10 nM, 15 nM, 17.5 nM) (D) The corresponding digital images.

in the concentration range from 0.2 nM to 17.5 nM ($R^2$ = 0.995). The detection limit can reach as low as 0.05 nM at a signal-to-noise ratio of 3, which is lower than many previous reports. In addition, we compared the detection limit and detection time of the reported method. Table 2 shows the comparison of different methods for abrin detection. The analytical parameters are comparable or even better than those reported in the literature. The previous methods suffer from some disadvantages. A SERS assay,[9] an electrochemiluminescence assay[10] and an LC/MS assay[11] rely on sophisticated instruments. An enzyme linked immunosorbent assay[12,13] requires a specific antibody against the analyte, which demands high cost and time consuming work. An aptamer-based fluorescent biosensor strategy[30] needs an aptamer to be labeled with signal materials and the introduction of a labeling substance makes the assay more complicated, time consuming and laborious, while our aptamer-based colorimetric biosensor assay only needs cheap instrument and simple design, and can be performed in the absence of a trained technician. In addition, our strategies do not need an aptamer to be labeled with signal materials. Thus the assay has the advantages of convenience, low cost, time saving and the ease of operation.

### 3.5. Selectivity

The developed aptamer-based colorimetric biosensor is also specific. To evaluate this property, we challenged the system with the target abrin (5 nM) and several non-targeted proteins such as thrombin (Th), glucose oxidase (GOx), and bovine serum albumin (BSA) (all at 5 nM). Fig. 4 shows that $\Delta A$ at 650 nm in the presence of abrin is considerably larger than

Table 2 Comparison of different methods for abrin detection

| Detection method | Detection limit | Detection time (including pre-treatment time) |
|---|---|---|
| SERS assay[9] | 0.1 ng mL$^{-1}$ | 11.5 h |
| Electrochemiluminescence assay[10] | 0.5 ng mL$^{-1}$ | 17 h |
| Enzyme linked immunosorbent assay[12] | 7.8 ng mL$^{-1}$ | 15 h |
| LC/MS assay[11] | 25 ng mL$^{-1}$ | Not given |
| Enzyme linked immunosorbent assay[13] | 35 ng mL$^{-1}$ | 15 h |
| Aptamer-based fluorescent biosensor assay[30] | 60.8 ng mL$^{-1}$ | Not given |
| Aptamer-based colorimetric biosensor assay (this work) | 0.05 nM (2.5 ng mL$^{-1}$) | 1 h |

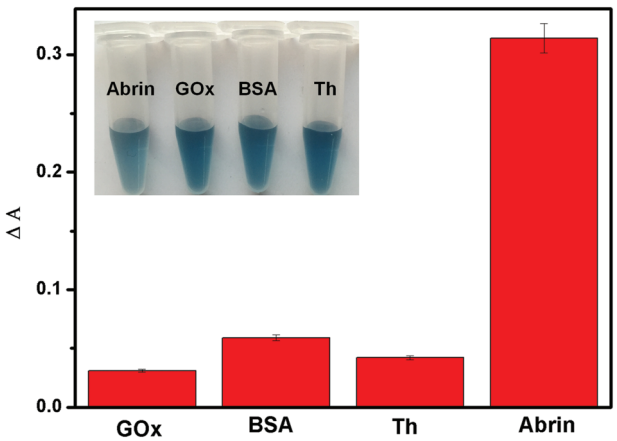


Fig. 4 The selectivity of the proposed system towards abrin detection. The concentration of abrin and other proteins is 5 nM. Inset shows the corresponding digital images.

those of other proteins. The results indicate that our approach has a high specificity to abrin.

### 3.6. Application in practical samples

In order to evaluate the feasibility of the present method in practical applications, the detection of abrin in raw milk was carried out. The practical samples were spiked with certain amounts of abrin. Table 3 shows that the recoveries of the practical samples are in the range 96.5% to 110.0%. The desirable recoveries demonstrate the reliability of the proposed method for detection of abrin in practical applications.

Table 3 Analytical results for abrin in raw milk samples

| Sample | Add (nM) | Found[a] (nM) | Recovery (%) | RSD (%) |
|---|---|---|---|---|
| Raw milk 1 | 3.0 | 3.3 ± 0.04 | 110.0 | 1.36 |
| Raw milk 2 | 17.5 | 16.9 ± 0.2 | 96.5 | 1.18 |

[a] Average of three determinations ± standard deviation.

## 4. Conclusions

In summary, we have successfully developed a sensitive, accurate and reliable aptamer-based colorimetric biosensor for the determination of abrin based on peroxidase-like activity of gold nanoparticles without complicated modification and expensive instruments. The dark-blue to light-blue color change in the presence of abrin was found to be easily observed by the naked eye or measured by using a UV-vis spectrometer. The linear range and its detection limit were found to be 0.2 nM to 17.5 nM and 0.05 nM, respectively. More importantly, the proposed method has been successfully applied to the detection of abrin in practical samples. Therefore, this method may offer a new approach for developing simple, low cost and sensitive sensors for abrin detection.

## Acknowledgements

Financial support from the National Basic Research Program of China (973 program, no. 2010CB933600) and the National Natural Science Foundation of China (21275135 and 21405146) is gratefully acknowledged.

## Notes and references

1 J. Cheng, T. H. Lu, C. L. Liu and J. Y. Lin, *J. Biomed. Sci.*, 2010, **17**, 34.
2 K. Dickers, K. Bradberry, P. Rice, G. Griffiths and J. A. Vale, *Toxicol. Rev.*, 2003, **22**, 137–142.
3 S. Bradberry, K. Dickers, P. Rice, P. Griffiths and J. A. Vale, *Toxicol. Rev.*, 2003, **22**, 65–70.
4 S. Olsnes, K. Refsnes and A. Pihl, *Nature*, 1974, **249**, 627.
5 Y. Endo, K. Mitsui, M. Motizuki and K. Tsurugi, *J. Biol. Chem.*, 1987, **262**, 5908.
6 G. D. Griffiths, M. D. Leek and D. J. Gee, *J. Pathol.*, 1987, **151**, 221.
7 J. N. Hughes, C. D. Lindsay and G. D. Lindsay, *Hum. Exp. Toxicol.*, 1996, **15**, 443.
8 X. B. Li, W. Yang, Y. Zhang, Z. G. Zhang, T. Kong, D. N. Li, J. J. Tang, L. Liu, G. W. Liu and Z. Wang, *J. Agric. Food Chem.*, 2011, **59**, 9796–9799.

9 H. Yang, M. Deng, S. Ga, S. H. Chen, L. Kang, J. H. Wang, W. W. Xin, T. Zhang, Z. R. You, Y. An, J. L. Wang and D. X. Cui, *Nanoscale Res. Lett.*, 2014, **9**, 138.
10 E. A. E. Garber, J. L. Walker and T. W. O'Brien, *J. Food Prot.*, 2008, **71**, 1868–1874.
11 J. Owens and C. Koester, *J. Agric. Food Chem.*, 2008, **56**, 11139–11143.
12 X. B. Li, W. Yang, Y. Zhang, Z. G. Zhang, T. Kong, D. N. Li, J. J. Tang, L. Liu, G. W. Liu and Z. Wang, *J. Agric. Food Chem.*, 2011, **59**, 9796–9799.
13 H. Y. Zhou, B. Zhou, H. Z. Ma, C. Carney and K. D. Janda, *Bioorg. Med. Chem. Lett.*, 2007, **17**, 5690–5692.
14 A. D. Ellington and J. W. Szostak, *Nature*, 1990, **346**, 818–822.
15 T. Kunii, S. Ogura, M. Mie and E. Kobatake, *Analyst*, 2011, **136**, 1310–1312.
16 J. Lee, M. Jo, T. H. Kim, J. Y. Ahn, D. K. Lee, S. Kim and S. Hong, *Lab Chip*, 2011, **11**, 52–56.
17 R. L. Srinivas, S. C. Chapin and P. S. Doyle, *Anal. Chem.*, 2011, **83**, 9138–9145.
18 C. Tuerk and L. Gold, *Science*, 1990, **249**, 505.
19 W. Yuanboonlim, W. Siripornnoppakhun, N. Niamnont, P. Rashatasakhon, T. Vilaivan and M. Sukwattanasinitt, *Biosens. Bioelectron.*, 2012, **33**, 17–22.
20 Y. Jv, B. Li and R. Cao, *Chem. Commun.*, 2010, **46**(42), 8017–8019.
21 S. Wang, W. Chen, A. Liu, L. Hong, H. Deng and X. Lin, *ChemPhysChem*, 2012, **13**(5), 1199–1204.
22 Z. Gao, M. Xu, L. Hou, G. Chen and D. Tang, *Anal. Chim. Acta*, 2013, **776**, 79–86.
23 H. Jiang, Z. Chen, H. Cao and Y. Huang, *Analyst*, 2012, **137**(23), 5560–5564.
24 X. Wang, Q. Wu, Z. Shan and Q. Huang, *Biosens. Bioelectron.*, 2011, **26**(8), 3614–3619.
25 J. Tian, Q. Liu, A. Asiri, A. Qusti, A. Al-Youbi and X. Sun, *Nanoscale*, 2013, **5**(23), 11604–11609.
26 Q. Chen, M. L. Liu, J. N. Zhao, X. Peng, X. J. Chen, N. X. Mi, B. D. Yin, H. T. Li, Y. Y. Zhang and S. Z. Yao, *Chem. Commun.*, 2014 (50), 6771–6774.
27 L. Gao, J. Gao, L. Nie, J. Zhang, Y. Zhang, N. Zhang, T. Wang, J. Wang, D. Wang, S. Perrett and X. Yan, *Nat. Nanotechnol.*, 2007, **2**(9), 577–583.
28 M. Comotti, C. Della Pina, R. Matarrese and M. Rossi, *Angew. Chem., Int. Ed.*, 2004, **43**, 5812.
29 Y. Lin, Z. Li, Z. Chen, J. Ren and X. Qu, *Biomaterials*, 2013, **34**, 2600.
30 J. J. Tang, T. Yu, L. Guo, J. W. Xie, N. S. Shao and Z. K. He, *Biosens. Bioelectron.*, 2007, **22**, 2456–2463.
31 G. N. Mayer, *Nucleic Acid and Peptide Aptamers: Method and Protocols*, Humana, New York, NY, 2009.
32 M. M. Maye, L. Han, N. N. Kariuki, N. K. Ly, W. B. Chan, J. Luo and C.-J. Zhong, *Anal. Chim. Acta*, 2003, **496**, 17–27.
33 X. F. Li, J. Li, H. Y. Kuang, L. Feng, S. J. Yi, X. D. Xia, H. W. Huang, Y. Chen, C. R. Tang and Y. L. Zeng, *Anal. Chim. Acta*, 2013, **802**, 82–88.
34 F. Yu, Y. Huang, A. J. Cole and V. C. Yang, *Biomaterials*, 2009, **30**, 4716–4722.
35 Y. P. Liu and F. Q. Yu, *Nanotechnology*, 2011, **22**, 145704.
36 H. X. Li and L. J. Rothberg, *Anal. Chem.*, 2004a, **76**(18), 5414–5417.
37 H. X. Li and L. J. Rothberg, *J. Am. Chem. Soc.*, 2004b, **126**(35), 10958–10961.

 